Elucidation of the Mechanism for Intestinal Phosphate Absorption

January 2022

Yasuhiro ICHIDA

Elucidation of the Mechanism for Intestinal Phosphate Absorption

A Dissertation Submitted to

the Graduate School of Science and Technology,

University of Tsukuba

in Partial Fulfillment of Requirements

for the Degree of Doctor of Philosophy in Science

Doctoral Program in Biology

Degree Programs in Life and Earth Sciences

Yasuhiro ICHIDA

Table of contents

Contents

Abstract 1

Abbreviations 2

General Introduction 4

Chapter 1. Significant species differences in intestinal phosphate absorption between dogs, rats, and monkeys 5

1. Introduction 5

2. Materials and Methods 6

3. Results 10

4. Discussion 23

Chapter 2. Evidence of an intestinal phosphate transporter alternative to type IIb sodium-dependent phosphate transporter in rats with chronic kidney disease. 25

1. Introduction 25

2. Materials and Methods 25

3. Results 31

4. Discussion 31

General Discussion 53

Acknowledgements 55

References 56

List of Publications 61

Abstract

Phosphate is an essential element for all animals and blood phosphate concentration is controlled strictly. Blood phosphate concentration is regulated by absorption from small intestine and excretion from kidney, and kidney plays an important role in maintaining the concentration. However, when renal function declines, phosphate excretion into urine is suppressed. Therefore, many patients with chronic kidney disease (CKD) and dialysis present with hyperphosphatemia. Phosphate binders that suppress phosphate absorption from the gastrointestinal tract are widely used for the treatment of hyperphosphatemia, but the development of new drugs for hyperphosphatemia is required in terms of dose, accumulation of metal adsorbents in the body, and gastrointestinal disorders of polymer adsorbents.

Na-dependent phosphate transporter type IIb (Slc34a2, NaPi-IIb) is considered to be the main target for the treatment of hyperphosphatemia for phosphate absorption from the small intestine. However, in recent years, ASP3325, which was developed as a NaPi-IIb selective inhibitor, has not been confirmed to be effective in clinical trials for hyperphosphatemia. In addition to NaPi-IIb, type III (Slc20a1, PiT-1 and Slc20a2, PiT-2) has been reported to exist in the small intestine as a transporter involved in phosphate absorption. However, many of the phosphate absorption mechanisms in the gastrointestinal tract, such as the contribution rate of these transporters and fluctuations in biological conditions, are unknown. In addition, it is known that there is a large difference in the expression distribution of NaPi-IIb between mice and rats, and it is thought that there is a species difference in phosphate absorption from the small intestine, but it is optimal for extrapolation of humans. There has been little discussion of various animal species so far. It is important to clarify these points in the development of therapeutic drug for human hyperphosphatemia. In this study, I examined (1) species differences in the mechanism of small intestinal phosphate absorption in experimental animals, and (2) changes in the contribution rate of each transporter involved in small intestinal phosphate absorption due to physiological changes during aging and nephropathy. With aging, the demand for phosphate decreased and the expression level of NaPi-IIb also decreased. On the other hand, during renal injury, as the expression of NaPi-IIb in the small intestine decreased, the contribution of PiT-1, which had a lower affinity for phosphate than NaPi-IIb, for phosphate absorption in the small intestine increased. From these results, a new mechanism of small intestinal phosphate absorption different from that of NaPi-IIb derived from PiT-1 was clarified. It is important to inhibit not only NaPi-IIb but also PiT-1 / 2 mediated

phosphate absorption in the suppression of phosphate absorption in the small intestine for the purpose of treating hyperphosphatemia.

Abbreviations

ALP:	alkaline phosphatase
BBMV:	brush border membrane vesicles
CKD:	chronic kidney disease
FGF23:	fibroblast growth factor 23
LC-MS/MS:	liquid chromatography-tandem mass spectrometer
NaPi-IIb:	Na-dependent phosphate transporter type IIb (Slc34a2)
PiT-1:	NaPi-IIb, type III (Slc20a1)
PiT-2:	NaPi-IIb, type III (Slc20a2)
PTH:	parathyroid hormone
UN:	urea nitrogen

General Introduction

Phosphate is essential for all livings. It exists in tissues and cells in the body and is also a component of cell membranes and bones, and nucleic acid substances such as DNA and RNA. Changes in blood phosphate concentration always have a large effect on the body and need to be controlled to be constant. Blood phosphate concentration in healthy individuals is regulated by absorption from the small intestine, release and utilization from bone, and excretion from the kidney. Among them, the kidney plays an important role in maintaining its blood concentration. However, when renal function is severely reduced, phosphate excretion into urine is suppressed. Therefore, many patients with chronic kidney disease (CKD) and dialysis present with hyperphosphatemia. Hyperphosphatemia is accompanied by cardiovascular disorders associated with ectopic calcification, and its cardiovascular events are the leading cause of death in dialysis patients. A phosphate binder that suppresses phosphate absorption from the digestive tract is widely used for the treatment of hyperphosphatemia. However, since these drugs dose are high, there is a problem in compliance, and the development of new drugs is required from the viewpoint of accumulation of metal-type adsorbents in the body and gastrointestinal disorders of polymer-type adsorbents.

Rodent studies have revealed that sodium-dependent phosphate transporter type IIb (Slc34a2, NaPi-IIb) plays a major role in small intestinal phosphate absorption, and it is considered as a target for the treatment of hyperphosphatemia. However, in recent years, ASP3325, which was developed as a selective inhibitor of NaPi-IIb, has not been confirmed to be effective in clinical trials for hyperphosphatemia in CKD patients. In addition to NaPi-IIb, type III (Slc20a1, PiT-1 and Slc20a2, PiT-2) exists in the small intestine as transporters involved in phosphate absorption. However, many of the small intestinal phosphate absorption mechanisms, such as the contribution rate of these transporters are unknown. In addition, it is known that there is a large difference in the expression distribution of NaPi-IIb between mice and rats, and it is thought that there is a species difference in small intestinal phosphate absorption, it is an optimal animal for extrapolation of humans. Little discussion has been made about species so far. It is important to clarify these points in the development of drugs for human hyperphosphatemia. In this study, I examined (1) species differences in the mechanism of small intestinal phosphate absorption in experimental animals, and (2) changes in the contribution rate of each transporter involved in small intestinal phosphate absorption due to physiological changes during aging and CKD.

Chapter 1. Significant Species Differences in Intestinal Phosphate Absorption between Dogs, Rats, and Monkeys.

1. Introduction

Blood phosphate levels are regulated by absorption in the intestines, release and utilization by bones, and excretion from kidneys. Among them, the kidney plays an important role in regulating blood phosphate concentration, which is maintained by adjusting the urinary excretion of phosphate (1). Phosphate excretion into urine is performed via reabsorption by NaPi-IIa and NaPi-IIc in kidneys, and FGF23 negatively regulates the translocation of NaPi-IIa and NaPi-IIc into the renal tubular epithelium (2). However, in patients with chronic kidney disease (CKD) and/or dialysis, urinary phosphate excretion decreases remarkably as kidneys fail to remove dietary phosphate from the body, leading to hyperphosphatemia (3). Hyperphosphatemia causes secondary hyperparathyroidism and vascular calcification, which are known risk factors for death or a decline in the quality of life (4, 5). Phosphate binders are used in patients with hyperphosphatemia to suppress phosphate absorption in the gastrointestinal tract (6-8). In patients with CKD and/or dialysis, blood phosphate levels are strongly influenced by uptake in the small intestine (9, 10).

Dietary phosphate is composed of organic phosphates and phosphoric acid, an inorganic phosphate. Organic phosphate is metabolized into phosphoric acid by alkaline phosphatase (ALP) in the digestive tract (11). In the gastrointestinal tract this phosphate is absorbed. There are two pathways of phosphate absorption in the small intestine, active transport via intestinal epithelial cells and passive transport via the tight junction between cells. Little is known about the contribution between passive flow from tight junction and active transport, but active transport has been thought to play an important role in maintaining phosphate absorption in the small intestine (12-14). In humans and rats, the active transport of phosphate mainly happens in the upper part of the small intestine where NaPi-IIb, a sodium-dependent phosphate transporter, is thought to have an important function (15-18). However, it was reported that the efficacy of a NaPi-IIb specific inhibitor was different between rats and humans (19). And NaPi-IIb is also active in mice, but mainly in the lower part of the small intestine (15, 16, 20). These reports indicate that there are species differences in the intestinal phosphate absorption system among rats, mice, and humans. NaPi-IIb which has a strong affinity for phosphate is highly expressed in the small intestine, and it is well known that NaPi-IIb is regulated by $1,25(OH)_2D_3$ in rodents, $1,25(OH)_2D_3$ administration or $1,25(OH)_2D_3$ receptor deletion causes the increase or decrease of NaPi-IIb protein expression, respectively (21,22). However, the expression of PiT-1 and PiT-2,

together known as NaPi-III, in addition to NaPi-IIb have also been confirmed in the small intestine. As PiT-1 and PiT-2 are thought to be low affinity transporters for phosphate, while NaPi-IIb has high affinity, the characteristic difference of these transporters might be physiological meaning. (12, 23).

Rats, dogs, and monkeys are widely used for the prediction of drug efficacy and toxicity in humans. In choosing an animal model to predict the effect of an inhibitor for phosphate absorption in the human small intestine, it is important to confirm the species difference. In this study, urinary and fecal phosphate excretion *in vivo*, phosphate uptake in the small intestine by brush border membrane vesicles (BBMV), and the expression levels of three intestinal sodium-dependent phosphate transporters were examined in rats, dogs and monkeys to confirm the species difference in phosphate absorption.

2. Materials and Methods

Animals. Animal procedures and protocols were in accordance with the Guidelines for the Care and Use of Laboratory Animals at Chugai Pharmaceutical Co. Ltd. and approved by the Institutional Animal Care and Use Committee (approval number: 17-073, 17-160, 17-264). Nine weeks old rats (Wistar), 2 years old dogs (Beagle) and 5 years old monkeys (Cynomolgus monkey) were included in the study. Rats were fed a 10 g pellet diet (CE-2, Japan CREA, Japan), dogs were fed a 200 g pellet diet (CD-5M, Japan CREA) and monkeys were fed a 100 g pellet diet (Certified Primate Diet 5048, LabDiet, MO, USA) per day. Phosphate, calcium, and vitamins in these diets were derived from soybeans and whitefish. The contents are as follows; CE-2: phosphate 1.1 g, calcium 1.1 g, vitamin D3 275 IU/100 g, CD-5M: phosphate 1.2 g, calcium 1.5 g, vitamin D3 265 IU/100 g, Certified Primate Diet 5048: phosphate 0.6 g, calcium 1.0 g, vitamin D3 670 IU/100 g. The animals were euthanized by exsanguination under isoflurane or ketamine anesthesia.

Biochemical analysis. For each animal species, urine was collected for 24 hours and feces was stored for 48 hours. Feces samples were suspended in 0.5 mol/L hydrochloric acid (HCl) and centrifuged to collect the supernatant (15 min, 1,630 × g, 4℃). Urine samples were diluted with an equal amount of 1 mol/L HCl and centrifuged to collect the supernatant (15 min, 1,630 × g, 4℃). Blood samples were centrifuged to collect serum (15 min, 1,630 × g, 4℃). Concentrations of phosphate (IATRO LQ IP II, LSI Medical Corporation, Japan), calcium (IATROFINE Ca II, LSI Medical Co.), creatinine (L type Wako creatinine, Wako Pure Chemical Industries, Ltd., Japan) and urea nitrogen (L type Wako UN, Wako Pure Chemical Industries, Ltd.) were measured by TBA2000 (TOSHIBA Co., Japan). Serum were stored and measured for $1,25(OH)_2D_3$ (FR, FUJIREBIO Inc., Japan) and FGF23 (FGF-23 ELISA Kit, KAINOS Laboratories, Inc., Japan).

Preparation of BBMV and analysis of intestinal phosphate absorption, determination of protein concentration and the activity of alkaline phosphatase. The duodenum was sampled from stomach pylorus to Triez's ligament, jejunum was 10 or 15 cm descending from Triez's ligament, and ileum was 10 or 15 cm ascending from the cecum. These samples were washed with saline, and mucosal tissue was scraped with a slide glass to acquire material for mRNA measurement, BBMV purification, kinetic analysis and ALP analysis. BBMV purification was performed using small intestinal mucosa collected from each individual. BBMV was prepared by partially modifying the previous method (24). The purification of BBMV was confirmed by enrichment of ALP activity, which was more than 7 fold compared with the homogenized tissue. The isolated BBMV were suspended in an experimental buffer to give a final protein concentration of about 1 mg/ml. The final experimental buffer consisted of either 60 mmol/L Mannitol, 110 mmol/L NaCl, 10 mmol/L HEPES-Tris, pH 7.5 (Na buffer). Uptake in the absence of Na^+ was measured by substituting NaCl with KCl (K buffer). Protein concentration of homogenized suspension was measured using the Bradford method. The ALP activity of the homogenized suspension was measured (L type Wako ALP J2, Wako Pure Chemical Industries, Ltd.) with an automatic analyzer. KH_2PO_4 was added to the Na buffer for a final concentration of 1, 3, 10, 25, 50, 100 μmol/L. $H_3{}^{33}PO_4$ (PerkinElmer Co., Ltd., Waltham, MA USA) was further added to prepare a Na buffer or K buffer. BBMV suspension was added to above solution and incubated at room temperature for 1 minute. Immediately after the incubation, an ice-cold stop solution consisting of either 1.0 mmol/L KH_2PO_4, 150 mmol/L NaCl, or 10 mmol/L HEPES-Tris (pH 7.5) was added to terminate the reaction, and the whole amount was added to a 0.45 μm membrane filter (Merck Millipore, Burlington, MA USA). Radioactivity was measured using a liquid scintillation counter (PerkinElmer Co., Ltd.) and sodium dependent uptake was calculated by deducting the uptake with K buffer.

Gene expression. Using the small intestinal mucosa of each collected individual, mRNA was purified using RNeasy kit (RNeasy kit, QIAGEN, Venio, Netherlands). cDNA was prepared using SuperScript IV (Life Technology Japan, Ltd., Japan). Expression of mRNA was measured by real-time PCR (TaqMan Universal PCR Mix, Life technology Japan, Ltd., Advanced Universal Probes Supermix, Bio-Rad Laboratories, Inc., Hercules, CA USA). The cDNA fragments of the target sequences were generated by RT-PCR with specific primers from the total intestinal RNA of each species. Each cDNA fragment was ligated into the pcDNA3.1 vector (Life technology Japan, Ltd.). Reference sequence and gene localization of each cDNA fragment are shown in Table 1. The concentrations of the purified plasmid DNA were measured by spectrophotometry, and corresponding copy numbers were calculated. Serial dilutions of the respective plasmid DNA were used as standards to make

calibration curves. At that time, the plasmids containing the mRNA sequence corresponding to the real-time PCR probe (Life technology Japan, Ltd., Bio-Rad Laboratories, Inc.) of NaPi-IIb, PiT-1, PiT-2, and Villin-1 were used as a standard, and the absolute amount of mRNA of each gene was calculated from a calibration curve.

Table 1. The amplified DNA sequences used for the analysis of NaPi-IIb, PiT-1, PiT-2, and Villin-1 mRNA expression level.

	cDNA target	Reference sequence	Gene localization
Rat	NaPi-IIb	NM_053380	601 - 730
	PiT-1	NM_031148	511 - 740
	PiT-2	NM_017223	601 - 810
	Villin-1	NM_001108224	391 - 540
Dog	NaPi-IIb	XM_022417261	387 - 478
	PiT-1	XM_540181	862 - 957
	PiT-2	XM_025993676	485 - 550
	Villin-1	XM_026002027	80 – 106
Monkey and human	NaPi-IIb	NM_006424	1006 - 1175
	PiT-1	NM_005415	2279 - 2408
	PiT-2	NM_001257180	982 - 1171
	Villin-1	NM_007127	2331 - 2540

Statistical analysis. Statistical analysis was performed using Microsoft Office Excel (Microsoft Corporation, Redmond, WA USA). The Michaelis-Menten curve was generated based on substrate concentration (s) (s = 1, 3, 10, 25, 50, 100 μmol/L) and calculated velocity (v), and the apparent Michaelis constant (Km) and maximum velocity ($Vmax$) of phosphate uptake were calculated nonlinearly with JMP 11. 2. 1 (SAS Institute Japan Ltd., Japan). For biochemical and gene expression, statistical analysis was performed using one-way ANOVA. Tukey–Kramer multiple comparison tests were used to compare data, with $p<0.05$ being considered statistically significant with JMP 11. 2. 1.

3. Results

Biochemical analysis of phosphate metabolisms in blood, urine, and feces

Serum biochemical data are shown in Table 2. Serum phosphate concentration was the highest in rats and lowest in dogs. There was no species difference in calcium concentration. Serum FGF23 concentration in dogs was markedly high, followed by rats. Serum $1,25(OH)_2D_3$ concentration was the highest in monkeys. Urinary biochemical data are shown in Table 3. Compared to rats and dogs, urinary phosphate excretion was remarkably low in monkeys and calcium excretion was markedly high. Fecal biochemical data are shown in Table 4. The intestinal phosphate absorption rate calculated based on the ratio of dietary to fecal phosphate was remarkably low in monkeys and the highest in dogs. Fecal calcium excretion was also the lowest in monkeys. It was comparable in rats and dogs.

Table 2. Serum phosphate, calcium, urea nitrogen, creatinine, FGF23, and 1,25(OH)2D3 levels in each species.

	Rat	Dog	Monkey	Human
Phosphate (mg/dL)	8.0 ± 0.1	3.3 ± 0.2[a]	4.7 ± 0.5[a, b]	3.4 ± 0.5
Calcium (mg/dL)	10.2 ± 0.1	10.1 ± 0.1	10.0 ± 0.2	9.3 ± 0.4
BUN (mg/dL)	10.1 ± 1.0	10.8 ± 0.6	24.0 ± 2.0[a, b]	
Creatinine (mg/dL)	0.23 ± 0.01	0.52 ± 0.01[a]	0.64 ± 0.06[a]	
FGF23 (pg/mL)	167.7 ± 9.6	553.8 ± 17.3[a]	67.4 ± 14.7[a, b]	69.7 (56.8 – 92.7)
$1,25(OH)_2D_3$ (pg/L)	94.2 ± 18.1	28.0 ± 4.7	218.8 ± 23.2	39.9 (30.2 – 49.6)

Values are expressed as means ± SE, n=4. [a]$p<0.05$, significant different from rat, [b]$p<0.05$, significant different from dog by one-way ANOVA and followed by Tukey–Kramer multiple comparison tests. Human data is referenced from a previous study (29).

Table 3. Urinary phosphate, calcium, urea nitrogen excretion, and the fractional excretion of phosphate in each species.

	Rat	Dog	Monkey	Human
Phosphate (mg/mg cre)	3.0 ± 0.1	1.8 ± 0.1[a]	0.01 ± 0.00[a, b]	
Calcium (mg/mg cre)	0.04 ± 0.00	0.08 ± 0.01[a]	0.65 ± 0.09[a, b]	
BUN (mg/mg cre)	11.5 ± 1.3	13.3 ± 0.3	9.9 ± 0.9[b]	
FEPi[1] (%)	8.6 ± 0.5	29.1 ± 1.3[a]	0.1 ± 0.1[a, b]	14.5 (11.9-20.1)

Values are expressed as means ± SE, n=4. [1]FEPi = fractional excretion of phosphate. [a]$p<0.05$, significant different from rat, b$p<0.05$, significant different from dog by one-way ANOVA and followed by Tukey–Kramer multiple comparison tests. Human data is referenced from a previous study (29).

Table 4. Fecal phosphate and calcium excretion and phosphate absorption rate in each species.

	Rat	Dog	Monkey	Human
Phosphate excretion[1] (mg/kg/day)	170 ± 4	128 ± 11[a]	120 ± 14[a]	
Calcium excretion[1] (mg/kg/day)	303 ± 29	335 ± 33	58 ± 9[a, b]	
Phosphate intake[1] (mg/kg/day)	322 ± 6	271 ± 3[a]	145 ± 20[a, b]	
Phosphate absorption rate[2] (%)	47.1 ± 0.9	52.7 ± 4.3	13.2 ± 14.0[a, b]	60 - 70

Values are expressed as means ± SE, n=4. [1]Phosphate excretion, calcium excretion and phosphate intake were corrected by body weight. [2]Phosphate absorption rate was calculated from phosphate in food and feces, as follows (phosphate intake - phosphate excretion) / phosphate intake * 100 (%). [a]$p<0.05$, significant different from rat, [b]$p<0.05$, significant different from dog by one-way ANOVA and followed by Tukey–Kramer multiple comparison tests. Human data is referenced from a previous study (30).

Kinetics analysis of phosphate uptake in intestinal BBMV

Figs. 1-3 show the Na^+-dependent phosphate uptake concentration dependence curve in each vesicle prepared from duodenum, jejunum, and ileum of three species. Kinetic parameters are shown in Table 5. The apparent *Km* for phosphate uptake in duodenum, jejunum, and ileum was 39.9, 78.9, 367.3 μmol/L in rats, 46.9, 14.4, 8.9 μmol/L in dogs and 31.6, 102.3, 44.9 μmol/L in monkeys, respectively. Dogs showed high *Vmax* at any site in small intestine. The relative contribution rate (*Vmax*/*Km*) at each site was the highest in the ileum in dogs and monkeys, and in the duodenum in the rats.

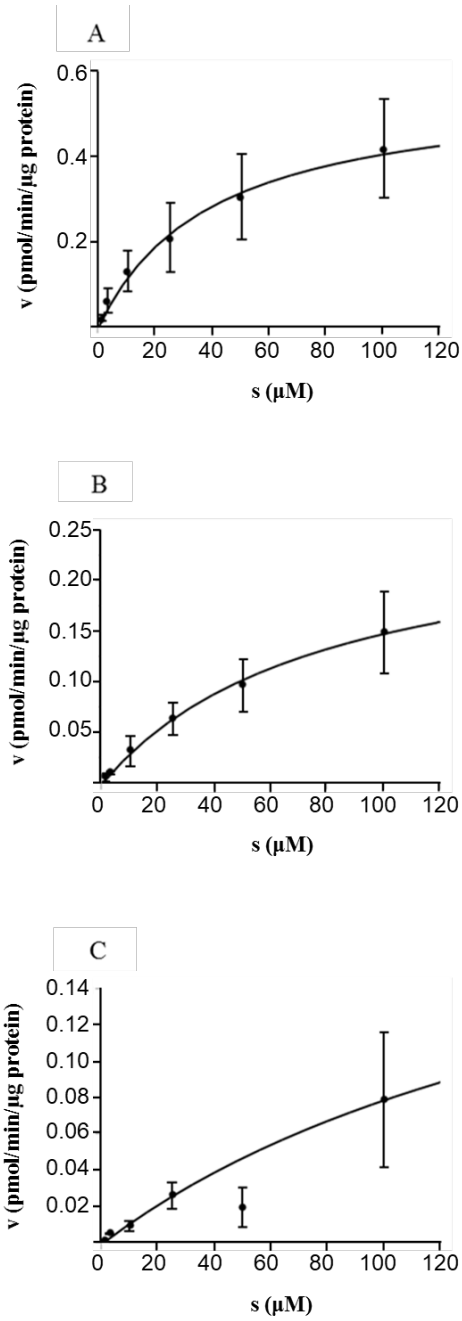

Figure 1. Michaelis-Menten curves of phosphate uptake in rats intestinal BBMV.
Values at each concentration are expressed as means ± SE, n=4. Phosphate uptake (v) was measured in the duodenum (A), jejunum (B), and ileum (C). BBMV treated with phosphate concentration (s) ranging from 1 to 100 μM for 1 min. Michaelis-Menten curves were analysed by JMP 11.2.1 using single kinetics model.

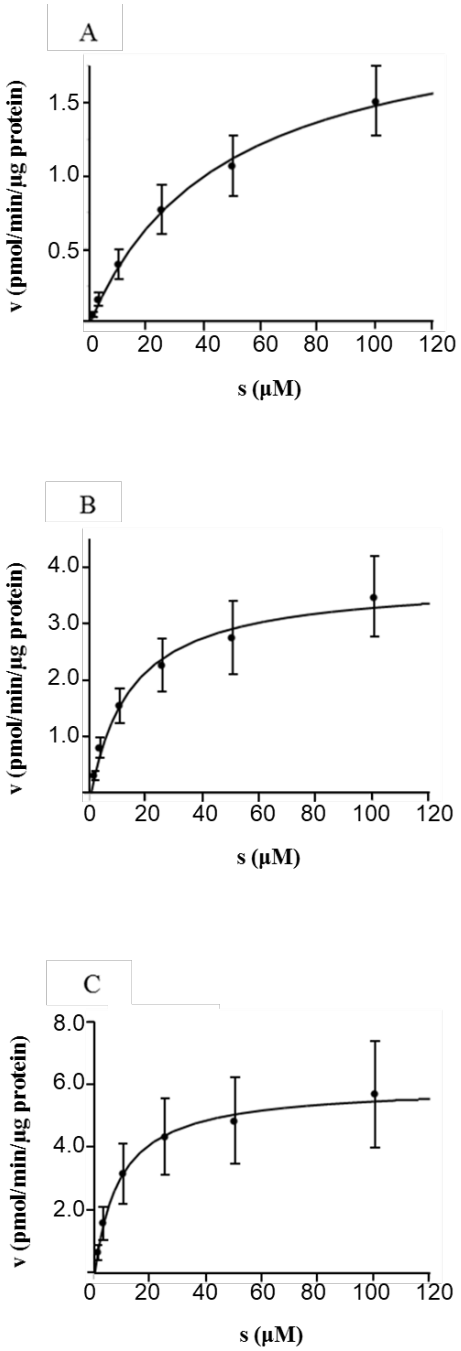

Figure 2. Michaelis-Menten curves of phosphate uptake in dogs intestinal BBMV. Values at each concentration are expressed as means ± SE, n=4. Phosphate uptake (v) was measured in the duodenum (A), jejunum (B), and ileum (C). BBMV treated with phosphate concentration (s) ranging from 1 to 100 μM for 1 min. Michaelis-Menten curves were analysed by JMP 11.2.1 using single kinetics model.

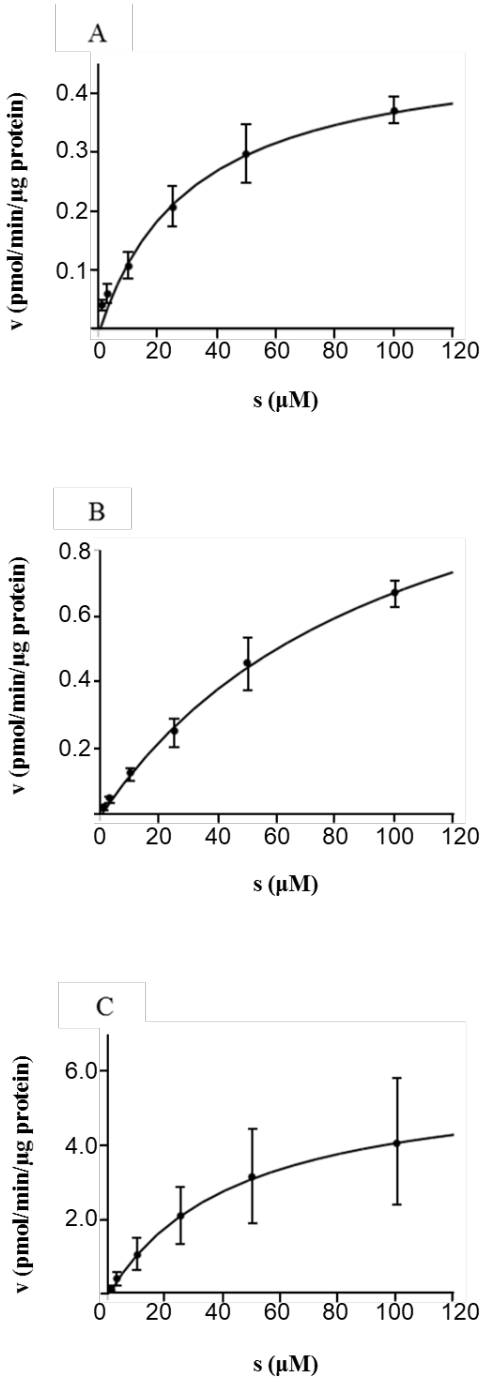

Figure 3. Michaelis-Menten curves of phosphate uptake in monkey intestinal BBMV. Values at each concentration are expressed as means ± SE, n=4. Phosphate uptake (v) was measured in duodenum (A), jejunum (B), and ileum (C). BBMV treated with phosphate concentration (s) ranging from 1 to 100 μM for 1 min. Michaelis-Menten curves were analyzed by JMP 11.2.1 using single kinetics model.

Table 5. Michaelis-Menten kinetics parameters of intestinal phosphate uptake in BBMV in rats, dogs, and monkeys.

Rat

	Duodenum	Jejunum	Ileum
K_m (μM)	39.9	78.9	367.4
V_{max} (pmol/min/μg protein)	0.57	0.27	0.56
V_{max}/K_m (pmol/min/μg protein/μM)	0.014	0.003	0.002

Dog

	Duodenum	Jejunum	Ileum
K_m (μM)	46.9	14.4	8.9
V_{max} (pmol/min/μg protein)	2.2	3.8	6.0
V_{max}/K_m (pmol/min/μg protein/μM)	0.047	0.26	0.67

Monkey

	Duodenum	Jejunum	Ileum
K_m (μM)	31.6	102.3	44.9
V_{max} (pmol/min/μg protein)	0.49	1.4	5.9
V_{max}/K_m (pmol/min/μg protein/μM)	0.015	0.013	0.13

Data was analyzed by JMP 11.2.1 using velocity and phosphate concentration in each species. *Vmax* represents the maximum absorption velocity of phosphate, *Km* is the Michaelis-Menten constant, which were obtained by fitting the experimental data into nonlinear least squares regression.

mRNA expression of NaPi-IIb, PiT-1 and PiT-2 in intestine

NaPi-IIb mRNA was expressed most highly in the ileum in dogs, but in the duodenum in rats (Fig. 4). In rats, PiT-1 mRNA was highly expressed in ileum, but PiT-2 mRNA was poorly expressed in all segments. In dogs, the mRNA expression of PiT-1 and PiT-2 was similar in all tissues. NaPi-IIb mRNA expression in monkeys was barely detectable in every part of the intestine, but contrastingly mRNA expression of PiT-1 and PiT-2 was confirmed (Fig. 4). In humans, expression of NaPi-IIb, PiT-1, and PiT-2 were evaluated using the Human Digestive System MTC ™ Panel (Clontech Laboratories, Inc., Mountain View, CA USA). NaPi-IIb was higher in the duodenum than in the rest of the human small intestine, but expression levels of PiT-1 and PiT-2 were similar (Fig. 5).

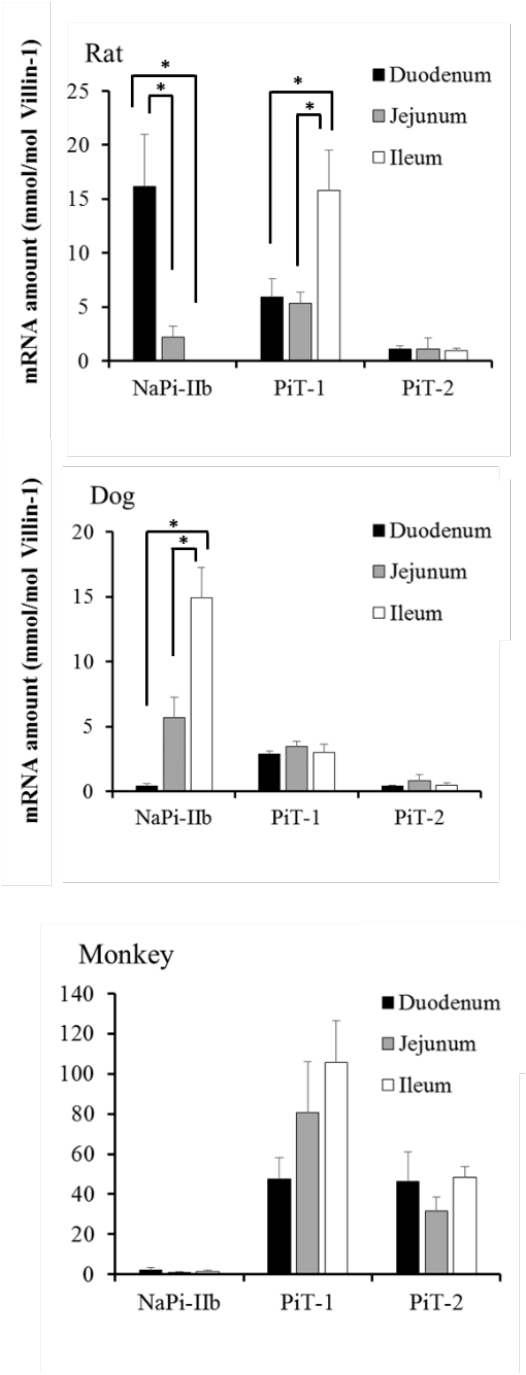

Figure 4. Intestinal NaPi-IIb, PiT-1 and PiT-2 mRNA expression in rats (A), dogs (B), and monkeys (C). The NaPi-IIb, PiT-1, and PiT-2 mRNA amount in each tissue was quantified by real-time PCR using the standard template DNA. cDNA were synthesized using mRNA purified from each tissue, and all values obtained were expressed as molecules per Villin-1 amount. All cDNA copy numbers were derived based on the same standard dilutions. Values are expressed as means ± SE, n=4. * $p<0.05$, significant difference by one-way ANOVA and followed by Turkey–Kramer multiple comparison tests.

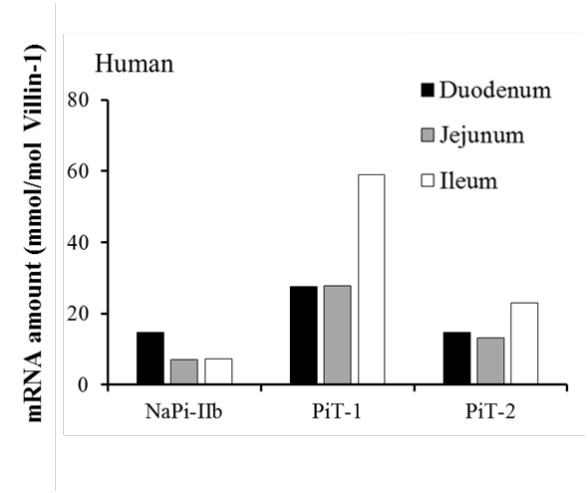

Figure 5. NaPi-IIb, PiT-1 and PiT-2 mRNA expression in each tissue measured by a commercial cDNA panel. Commercial pooled samples were used (duodenum pooled from 30 male/female Caucasians, ages 17-75, jejunum pooled from 6 male/female Caucasians, ages 20-57, ileum pooled from 8 male/female Caucasians, ages 18-57; Human Digestive System MTC™ Panel, Takara Bio Inc., Japan). All values obtained were expressed as molecules per Villin-1 amount. All cDNA copy numbers were derived based on the same standard dilutions.

Intestinal ALP activity

ALP activity in monkeys was lower than in dogs and rats (Fig. 6). In rats and dogs, organic phosphate is decomposed in the upper part of intestine, and thus ALP activity is high in the duodenum and jejunum.

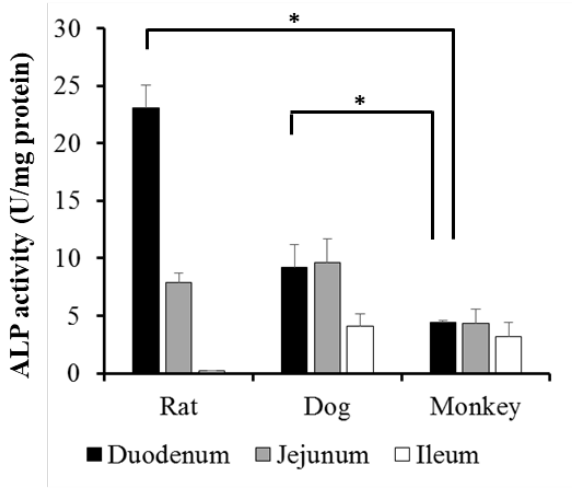

Figure 6. ALP activity in the duodenum, jejunum and ileum of each species. ALP activity of intestinal mucosa suspension was measured by a cyclic enzymatic amplification method. The values are expressed as means ± SE, n=4. * $p<0.05$, significant difference by one-way ANOVA and followed by Turkey–Kramer multiple comparison tests.

4. Discussion

In this study, I confirmed significant differences between rats, dogs, and monkeys in the absorption of phosphate. NaPi-IIb would contribute largely to phosphate uptake by BBMV in the small intestine of dogs and rats, whereas PiT-1 or PiT-2 would play that role in monkeys. Although monkey intestine is at least capable of the absorption of phosphate, the in vivo absorption and ALP activity was surprisingly low compared with dogs and rats, suggesting that the use of phosphate is much lower in monkeys.

BBMV analysis confirmed sodium-dependent phosphate uptake capacity in dogs, monkeys, and rats. In rats, NaPi-IIb was highly expressed in the duodenum, where the *Vmax/Km* ratio in BBMV was also the highest. These results suggest that the uptake of phosphate by NaPi-IIb in rats is most common in the duodenum. In contrast, in dogs, the *Vmax/Km* ratio and high expression of NaPi-IIb mRNA suggests more uptake in the ileum. These results suggest that phosphate uptake mainly occurs in ileum and that NaPi-IIb primarily contributes to this in dogs. In monkeys, the ileum was mainly involved in phosphate uptake based on the value of *Vmax/Km*. However, unlike in dogs and rats, not NaPi-IIb but PiT-1 and PiT-2 are mainly expressed in intestine in monkeys. This suggests that in monkeys, PiT-1 or PiT-2 contributes to phosphate uptake in the ileum.

It is known that NaPi-IIb in the small intestine is controlled by $1,25(OH)_2D_3$, and it has been reported that the expression of NaPi-IIb is increased by administration of $1,25(OH)_2D_3$ or ED-71 (21, 25, 26). However, in monkeys, despite having higher serum $1,25(OH)_2D_3$ than rats or dogs, PiT-1 and PiT-2 were highly expressed in each intestinal segment of monkeys, there is no correlation between BBMV phosphate uptake and the absolute mRNA amount of PiT-1 and PiT-2 in duodenum, jejunum and ileum. Another sodium-dependent phosphate transporter identified by Candeal et al. (27) may also be involved in monkeys. The verification of protein expression level and membrane localization of PiT-1 or PiT-2 will be required to confirm this in future studies.

In monkeys, the phosphate absorption rate calculated from diet and fecal excretion was significantly lower than in dogs and rats. ALP activity in the small intestine was also lower. When ALP activity is low, organic phosphate cannot be sufficiently decomposed into phosphoric acid in enough amounts. This suggests that while monkeys are capable of phosphate uptake in the small intestine, only small amounts of phosphate can be absorbed in the physiological condition. It remains unknown if systemic phosphate is supplied from intestine in an inorganic or organic form.

In addition to species differences in intestinal phosphate absorption, differences in the fractional urinary excretion of phosphate were also observed. Urinary phosphate excretion is mediated through reabsorption by renal NaPi-IIa and NaPi-IIc, and FGF23 negatively

regulates the internalization and degradation of NaPi-IIa and NaPi-IIc in the renal tubular epithelium (2). In dogs, urinary excretion of phosphate would be accelerated to regulate the large amount of phosphate absorbed in the small intestine as a result of high FGF23 concentration in the blood. In monkeys, the absorption of phosphate in the small intestine was low, and it was confirmed that serum FGF23 was also low and that reabsorption in kidneys was enhanced.

In humans, phosphate is reported to be mainly absorbed in upper intestine (28). High phosphate uptake in the duodenal BBMV of rats suggests that, compared with monkeys and dogs, rats should be the first choice for predicting phosphate metabolism in humans. However, I confirmed differences between humans and rats in the mRNA expression of PiT-1 and PiT-2 in the small intestine. The contribution of PiT-1 and PiT-2 to phosphate absorption in the small intestine remains unknown. NaPi-IIb specific inhibitor ASP3325 ameliorates the hyperphosphatemia in rats but is not effective in ESRD patients (19). It was suggested that not only NaPi-IIb but also PiT-1 and PiT-2 might relate with intestinal phosphate absorption. More research is necessary to confirm the validity of the rat model in predicting human responses.

In conclusion, dogs and monkeys absorb phosphate mainly in the lower intestine and rats in the upper part of the small intestine. NaPi-IIb mainly promotes uptake in dogs and rats, but other transporters besides NaPi-IIb do so in monkeys. Of the three species, dogs appear to absorb phosphate the most efficiently, and blood phosphate is maintained by high excretion in urine. Although monkeys possess active phosphate uptake mechanisms in the ileum, they could not utilize phosphate as much as the other species due to low ALP activity in the intestine. This study suggests that there are significant species differences among rats, dogs, and monkeys in the absorption of phosphate in the small intestine.

Chapter 2. Evidence of an intestinal phosphate transporter alternative to type IIb sodium-dependent phosphate transporter in rats with chronic kidney disease.

1. Introduction

Phosphate is absorbed in the small intestine by active transport via intestinal epithelial cells and passive flow via the tight junctions between cells (31). The sodium-dependent phosphate transporter NaPi-IIb, solute carrier family 34 member 2 (Slc34a2), was identified in the small intestine two decades ago (18). It is expressed mainly in intestine, lung, ovary, or testis and is thought to be involved in active intestinal phosphate absorption (17, 18, 32, 33). NaPi-IIb-deficient mice exhibit decreased intestinal phosphate absorption, low urinary phosphate excretion, low serum FGF23 levels, and increased serum calcitriol, all of which are consistent with systemic reductions of phosphate (15, 34, 38). In addition, the expression level of NaPi-IIb is correlated tightly with the active phosphate transport in rat intestinal brush-border membrane vesicles (BBMV) (26). Taken together, NaPi-IIb is thought to be the dominant intestinal phosphate transporter in rodents.

Hyperphosphatemia commonly develops in chronic kidney disease (CKD) due to impaired urinary phosphate excretion (35), and has been consistently associated with increased morbidity and mortality (5, 36, 37, 38). Phosphate binders are therefore recommended in such patients to reduce gastrointestinal phosphate absorption, since the intestinal absorption of phosphate is a major contributor to phosphate metabolism (7-10, 39). However, there is very little information about the intestinal expression level and activity of NaPi-IIb during kidney injury. Moreover, recent clinical trials in end stage renal disease patients revealed that the selective NaPi-IIb inhibitor ASP3325 neither inhibited intestinal phosphate absorption nor ameliorated hyperphosphatemia (19). Besides NaPi-IIb, there are other phosphate transporters in the intestine, specifically SLC20a family members PiT-1 (Slc20a1) and PiT-2 (Slc20a2) (12, 40), but their precise role in intestinal phosphate absorption in health and CKD remains unknown.

To resolve the above questions, I analyzed the correlation between the kinetics of active phosphate transport and the mRNA expression of NaPi-IIb, PiT-1, or PiT-2 in two rat models of CKD, namely adenine-induced nephropathy and anti-Thy1 nephritis. In addition, I adapted a highly sensitive liquid chromatography-tandem mass spectrometer (LC-MS/MS) method for simultaneous quantification of membrane proteins to determine the expression of NaPi-IIb (41).

2. Materials and Methods

Animal experiments

Male Wistar rats and Fischer 344 rats were purchased from Charles River Laboratories Japan, Inc. (Tokyo, Japan). Animal procedures and protocols were in accordance with the Guidelines for the Care and Use of Laboratory Animals at Chugai Pharmaceutical Co. Ltd. and approved by the Institutional Animal Care and Use Committee. For the analysis of healthy rats, 4, 9, and 15 week old Wistar rats were used. The adenine-induced CKD model was established by orally administrating adenine at 300 mg/kg to 6 week old Wistar rats for 4 weeks (5 times /week), after which they were subjected to analysis. Anti-Thy1-induced CKD was induced in 6 week old Fischer 344 rats as described (42). At 18 weeks after disease induction, animals were subjected to analysis. Rats had free access to food and to water. In the case of healthy rats and rats with anti-Thy1 CKD, they were fed CE-2 (CLEA Japan, inc., Tokyo, Japan), and CRF-1 (Oriental Yeast Co., Ltd., Tokyo, Japan) in the case of adenine CKD rats. The contents were as follows; CE-2: phosphate 1.1 g, calcium 1.1 g, vitamin D3 275 U per 100 g chow, CRF-1: phosphate 0.8 g, calcium 1.2 g, vitamin D3 643 U per 100 g chow. Alfacalcidol 0.2 μg/kg (Chugai Pharmaceutical Co. Ltd., Tokyo, Japan) or its vehicle (medium chain triglyceride) was administered by a single subcutaneous injection for 7 days. As phosphate is predominantly absorbed in duodenum and upper jejunum in rats (43), small intestinal samples were prepared by dissecting 10 cm of upper intestine starting at the pylorus. Preparation of brush border membrane vesicles (BBMV) for analyzing protein and phosphate uptake was carried out by partially modifying a previous method (32). The animals were euthanized by exsanguination under isoflurane or ketamine anesthesia.

Phosphate uptake in BBMV

The uptake of $H_3{}^{33}PO_4$ (PerkinElmer Co., Ltd., Waltham, MA) by BBMV was measured by a rapid filtration technique as described previously (44). Briefly, 80 μL of buffer containing specified concentrations of ^{33}P was added to 20 μL of membrane vesicles suspension. At the specified times the mixture was poured immediately onto Millipore filters (HAWP, 0.45 μm) and the radioactivity of the ^{33}P trapped in membrane vesicles was determined using a liquid scintillation counter (PerkinElmer Co., Ltd.). The buffer consisted of either 60 mmol/L mannitol, 110 mmol/L NaCl, 10 mmol/L HEPES-Tris, pH 7.5. Sodium-dependent phosphate uptake was calculated by deducting the uptake in buffer substituting NaCl with KCl. The Michaelis-Menten curve was generated based on substrate concentration and calculated velocity, and the apparent Michaelis constant (*Km*) and maximum velocity (*Vmax*) of phosphate uptake were calculated by a non-linear regression method using JMP 11.2.1 (SAS Institute Japan Ltd., Tokyo, Japan).

Measurement of NaPi-IIb, PiT-1, PiT-2 and Villin-1 mRNA by qPCR

Expression of mRNA was measured by qPCR using the Applied Biosystems 7900HT Fast Real-Time PCR System (Thermo Fisher Scientific K.K., Tokyo, Japan). The target sequences of NaPi-IIb, PiT-1, PiT-2, and Villin-1 for real-time PCR are listed in Table 6. The cDNA fragments of the target sequences were generated by reverse-transcribed PCR with specific primers from rat intestinal total RNA. Each PCR product was ligated into the pcDNA3.1 vector (Life Technologies Japan, Ltd.) and transformed into competent DH5α cells. The concentrations of purified plasmid DNA were measured by spectrophotometry and corresponding copy numbers were calculated. Serial dilutions of the respective plasmid DNA were used as standards to make calibration curves. The absolute amount of mRNA of each gene was calculated from the calibration curve and normalized by Villin-1.

Table 6. The amplified DNA sequences used for the analysis of NaPi-IIb, PiT-1, PiT-2, and Villin-1 mRNA expression level.

Molecule	GenBank Acc. No.	Location of amplification
NaPi-IIb	NM_053380	601 - 730
PiT-1	NM_031148	511 - 740
PiT-2	NM_017223	601 - 810
Villin-1	NM_001108224	391 - 540

Measurement of NaPi-IIb and Villin-1 protein by LC-MS/MS

BBMV of rat intestine was used to measure the protein of NaPi-IIb and Villin-1. The method was based on previous reports (41, 45). Briefly, intestinal samples were reduced and alkylated. Then the S-carbamoylmethylated proteins were digested. After adding stable isotope labeled internal standard peptides, the digests were extracted using OASIS MAX μElution plates (Waters Corporation, Milford, MA) and were analyzed by an ACQUITY UPLC M-class system coupled to a Xevo TQ-S triple quad mass spectrometer equipped with an ionKey system (Waters Corporation). The sequences used for the analyses are shown in Table 7.

Table 7. The amino acid sequences used for the analysis of NaPi-IIb, and Villin-1 protein expression level.

Molecule	Sequence	GenBank Acc. No.	Location
NaPi-IIb	VITDPFTK	NP_445832	266-273
Villin-1	YNDEPVQIR	NP_001101694	470-478

Biochemical analyses of rat serum

Serum phosphate, calcium, creatinine and urea nitrogen (BUN) were measured by an automatic analyzer (TOSHIBA Co., Tokyo, Japan). Calcitriol ($1,25(OH)_2D_3$ RIA Kit FR, Fujirebio, Inc., Tokyo, Japan) and FGF23 (FGF-23 ELISA Kit, KAINOS Laboratories, Inc., Tokyo, Japan) were measured according to the manufacturer's instructions.

Statistical analysis

Statistical analysis was performed using JMP 11.2.1. The Tukey-Kramer test was used for the aging rats study, and the Student's t-test for the CKD rats study.

3. Results

Intestinal phosphate uptake and transporters in healthy rats

I first examined the intestinal expression of phosphate transporters and intestinal phosphate metabolism in normal rats. Figure 7 shows sodium-dependent phosphate uptake in BBMV obtained from 4, 9, and 15 week old rats. Eadie–Hofstee plot analyses indicated that sodium-dependent uptake consisted of a single saturable component. Kinetic parameters calculated by the non-linear regression method are shown in Table 8. *Km* remained similar in rats aged 4, 9 and 15 weeks and the values corresponded to the *Km* of NaPi-IIb as reported previously (28). Vmax of rat intestinal phosphate transport markedly decreased with age (3.24, 1.12, and 0.47 pmol/μg protein/min, respectively).

The mRNA expression levels of the 3 intestinal phosphate transporters are shown in Table 9. PiT-2 mRNA levels were much lower than NaPi-IIb or PiT-1 in upper intestine. NaPi-IIb mRNA markedly decreased with age and paralleled the reduction of serum phosphate and calcitriol concentrations (Table 10) and phosphate uptake *Vmax* in BBMV (Table 8). On the other hand, PiT-1 mRNA did not change with age. Expression of NaPi-IIb protein was readily detected by the LC-MS/MS method, and corresponded to mRNA expression (Figure 8).

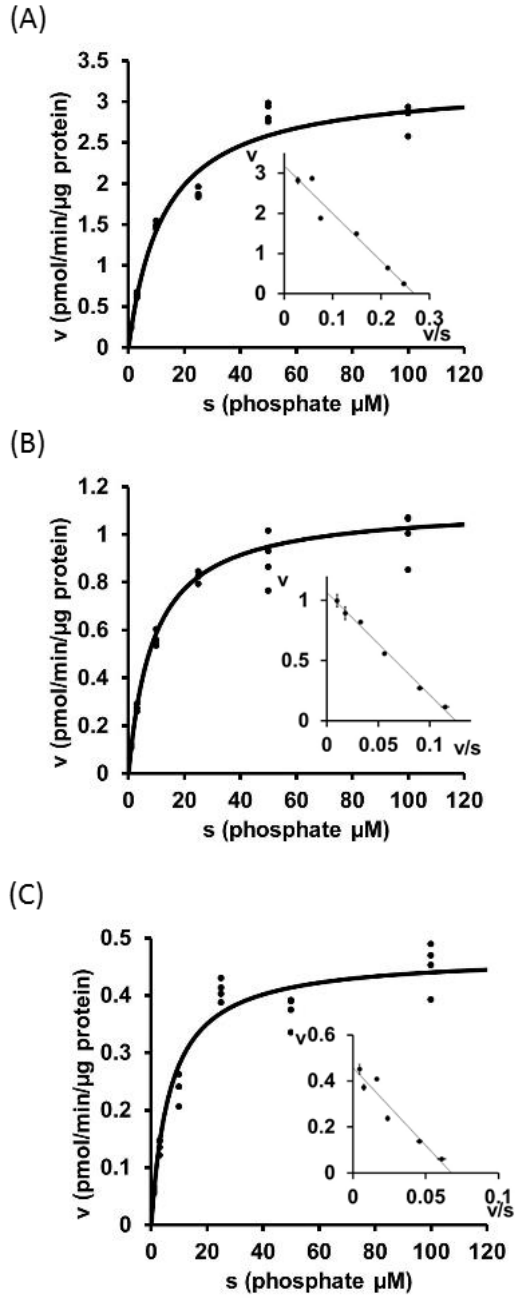

Figure 7. Changes in phosphate uptake by rat intestinal BBMV with age ((A) 4 wks old, (B) 9 wks old (C), 15 wks old). Dots represent the actual values and the Michaelis-Menten curve was generated using JMP11.2.1. Inset shows an Eadie-Hofstee plot of the uptake. Each point in the inset represents the mean of three measurement points.

(A)

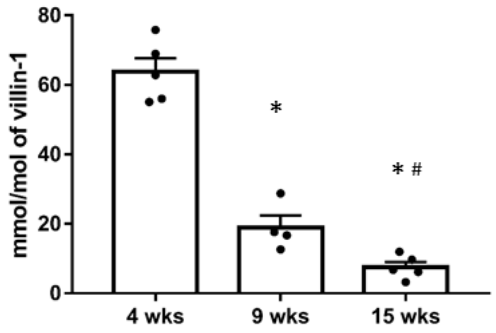

(B)

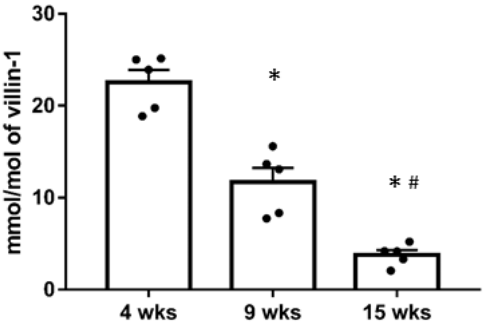

Figure 8. Changes in NaPi-IIb mRNA (A) or protein (B) expression level in rat upper intestine with age. Values are normalized by villin-1 protein or mRNA, respectively. The actual values are represented as dots, and the columns represent mean + SE. *$p<0.05$, significant difference versus 4wks old, #$p<0.05$, significant difference versus 9 wks old (Tukey-Kramer test).

Table 8. Kinetic parameters of phosphate uptake in rat BBMV with increasing age. Values are expressed as an estimate from non-linear regression analysis (n=4).

	4 wks old	9 wks old	15 wks old
K_m (μ mol/L)	12.6 (9.4 - 15.8)	9.0 (7.1 – 11.0)	6.8 (4.6 – 8.9)
V_{max} (pmol/min/μ g protein)	3.24 (3.00 - 3.47)	1.12 (1.05 – 1.18)	0.47 (0.42 – 0.50)

Values in parentheses are 95% confidence intervals.

Table 9. Changes in NaPi-IIb, PiT-1, or PiT-2 mRNA expression level in upper intestine with age in normal rats.

	4 wks old	9 wks old	15 wks old
NaPi-IIb (mmol/mol villin-1)	63.8 ± 3.9	18.9 ± 3.5[a]	7.6 ± 1.5[a, b]
PiT-1 (mmol/mol villin-1)	12.4 ± 2.0	9.2 ± 1.7	14.9 ± 1.8
PiT-2 (mmol/mol villin-1)	0.26 ± 0.05	0.17 ± 0.05	0.31 ± 0.12

Values are expressed as mean ± SE (n=12). [a]$p<0.05$, significant difference versus 4 wks old, [b]$p<0.05$, significant difference versus 9 wks old (Tukey-Kramer test).

Table 10. Serum biochemistry and phosphate-related hormones with age in normal rats.

	4 wks old	9 wks old	15 wks old
Phosphate (mg/dL)	9.6 ± 0.2	6.6 ± 0.2[a]	5.6 ± 0.1[a, b]
Calcium (mg/dL)	10.5 ± 0.1	10.4 ± 0.1[a]	10.1 ± 0.1[a, b]
BUN (mg/dL)	15.5 ± 0.5	18.1 ± 0.3[a]	17.9 ± 0.4[a, b]
Creatinine (mg/dL)	0.04 ± 0.01	0.07 ± 0.01[a]	0.15 ± 0.01[a, b]
FGF23 (pg/mL)	309 ± 34	457 ± 35[a]	689 ±60[a, b]
Intact PTH (pg/mL)	370 ± 22	279 ± 73[a]	167 ± 8[a, b]
Calcitriol (pg/mL)	311 ± 29	219 ± 16[a]	74 ± 12[a, b]

Values are expressed as mean ± SE (n=12). [a]$p<0.05$, significant difference versus 4 wks old, [b]$p<0.05$; significant difference versus from 9 wks old (Tukey-Kramer test).

Intestinal phosphate uptake and transporters in rats with adenine-induced CKD

Within 4 weeks, adenine-induced CKD in rats manifested as severe renal tubular injury accompanied by hyperphosphatemia, increased serum PTH and FGF23, and reduced calcitriol levels compared to normal rats (Table 11). Serum Ca did not change despite the calcitriol reduction at this point, but decreased as disease progressed further (data not shown). Figure 9 shows sodium-dependent phosphate uptake in intestinal BBMV prepared from normal and CKD animals. In contrast to healthy rats, where Eadie–Hofstee plot analysis indicated that intestinal phosphate uptake consisted of a single saturable component, it consisted of two saturable components in rats with adenine-induced CKD. Kinetic parameters calculated by the non-linear regression method are shown in Table 12. The *Km* values of normal rats and of the higher affinity component in CKD rats were 6.3 and 4.0 μmol/L, respectively, which is similar to the known *Km* of NaPi-IIb (46). The Km value of the lower affinity component in CKD rats was 166.1 μmol/L, similar to that of PiT-1 or PiT-2 as reported previously (47). The phosphate uptake *Vmax* of the higher affinity component in CKD rats was decreased compared to normal rats (0.23 versus 0.61 pmol/μg protein/min, respectively).

The mRNA expression levels of the 3 transporters are shown in Table 13. Similar to findings in healthy rats (see above), PiT-2 mRNA levels were much lower than NaPi-IIb or PiT-1 in upper intestine. Whereas PiT-1 and PiT-2 mRNA did not change in CKD rats compared to normal rats, the mRNA and protein expression level of NaPi-IIb, considered to be the main intestinal phosphate transporter in rats, significantly decreased in CKD rats compared to normal rats, mirroring the decrease of phosphate uptake velocity in adenine-induced CKD (Figure 10). The injection of alfacalcidol into CKD rats increased NaPi-IIb mRNA and protein expression back to normal levels (Table 14, Figure 7).

(A)

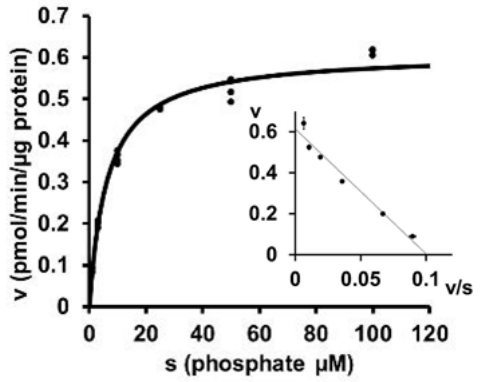

(B)

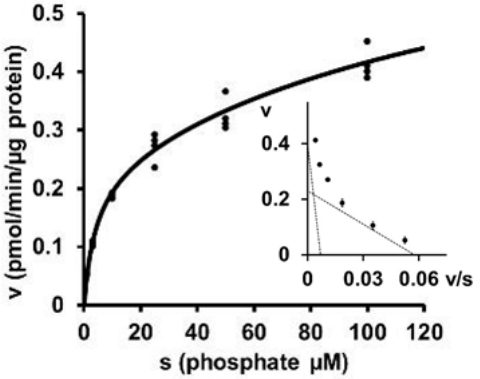

Figure 9. Phosphate uptake by intestinal BBMV in adenine-induced CKD rats. Dots represent the actual values and the Michaelis-Menten curve was generated using JMP11.2.1. Inset shows an Eadie–Hofstee plot of the uptake. Each point represents the mean of three measurement points. Normal: normal rats, CKD: adenine-induced CKD rats.

(A)

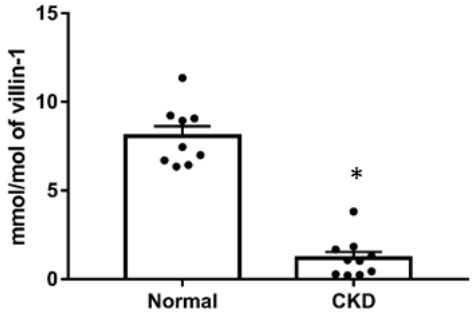

(B)

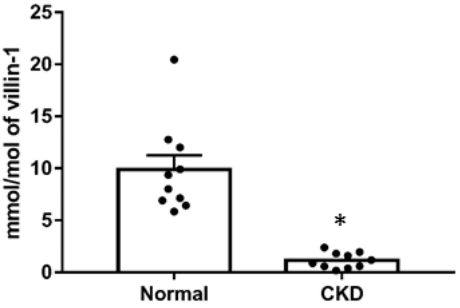

Figure 10. Changes in NaPi-IIb mRNA (A) or protein (B) expression level in upper intestine of rats with adenine-induced CKD. Values are normalized by villin-1 protein or mRNA, respectively. The actual values are represented as dots, and the columns represent mean + SE. *$p<0.05$, significant difference versus Normal (Student's t-test). Normal: normal rats, CKD: adenine-induced CKD rats.

Table 11. Serum biochemistry and phosphate-related hormones in rats with adenine-induced CKD.

	Normal	CKD
Phosphate (mg/dL)	7.1 ± 0.1	9.0 ± 0.4[a]
Calcium (mg/dL)	10.6 ± 0.1	10.7 ± 0.1
BUN (mg/dL)	21.2 ± 0.5	109.8 ± 5.5[a]
Creatinine (mg/dL)	0.26 ± 0.01	1.51 ± 0.09[a]
FGF23 (pg/mL)	1291 ± 170	14765 ± 2826[a]
Intact PTH (pg/mL)	143 ± 8	888 ± 117[a]
Calcitriol (pg/mL)	128 ± 16	14 ± 6[a]

Values are expressed as mean ± SE (n=10). [a]$p<0.05$, significant difference versus normal control rats (Student's t- test). Normal, normal rats; CKD, adenine-induced CKD rats.

Table 12. Kinetic parameters of phosphate uptake in BBMV of rats with adenine-induced CKD.

	Normal	CKD
K_m1 (μ mol/L)	6.3 ± 0.5	4.0 ± 1.7
$V_{max}1$ (pmol/min/ μ g protein)	0.61 ± 0.01	0.23 ± 0.06
K_m2 (μ mol/L)	-	166.1 ± 232.0
$V_{max}2$ (pmol/min/ μ g protein)	-	0.52 ± 0.32

Values are expressed as an estimate ± SE from non-linear regression analysis (n=4). Normal, normal rats; CKD, adenine-induced CKD rats.

Table 13. Changes in NaPi-IIb, PiT-1, or PiT-2 mRNA expression level in upper intestine in rats with adenine-induced CKD.

	Normal	CKD
NaPi-IIb (mmol/mol villin-1)	8.1 ± 0.5	1.2 ± 0.3[a]
PiT-1 (mmol/mol villin-1)	22.0 ± 2.0	22.7 ± 1.9
PiT-2 (mmol/mol villin-1)	0.21 ± 0.02	0.26 ± 0.05

Values are expressed as mean ± SE (n=10). [a]$p<0.05$, significant difference versus Normal (Student's t-test). Normal, normal rats; CKD, adenine-induced CKD rats.

Table 14. Changes in NaPi-IIb, PiT-1, or PiT-2 mRNA expression level in upper intestine in rats with adenine-induced CKD after subcutaneous administration of alfacalcidol.

	Normal	CKD	VitD
NaPi-IIb (mmol/mol villin-1)	8.1 ± 0.5	1.2 ± 0.3[a]	11.7 ± 1.86[b]
PiT-1 (mmol/mol villin-1)	22.0 ± 2.0	22.7 ± 1.9	19.6 ± 2.5
PiT-2 (mmol/mol villin-1)	0.21 ± 0.02	0.26 ± 0.05	0.23 ± 0.03

Values are expressed as mean ± SE (n=10). [a]$p<0.05$, significant difference versus Normal, [b]$p<0.05$, significant difference versus CKD (Student's t-test). Normal, normal rats; CKD, adenine-induced CKD rats, VitD, alfacalcidol via subcutaneous administration. Values were normalized via villin-1 mRNA.

Intestinal phosphate uptake and transporters in rats with anti-Thy1-induced CKD

Chronic anti-Thy1 nephritis, induced by anti-Thy1 antibody and uninephrectomy, was examined as another CKD model. Eighteen weeks after disease induction, serum creatinine, BUN, phosphate, intact PTH, and FGF23 significantly increased in diseased rats compared to sham-operated rats, whereas serum calcitriol decreased (Table 15). Similar to adenine-induced CKD, serum Ca did not change despite of the calcitriol reduction at this point, but decreased as the disease progressed (data not shown).

Figure 11 shows the sodium-dependent phosphate uptake in intestinal BBMV prepared from sham-operated and chronic anti-Thy1 CKD rats. As in adenine-induced CKD, Eadie–Hofstee plot analysis of anti-Thy1 induced rat CKD again revealed two saturable components (Table 16). *Km* of the higher affinity component in anti-Thy1 CKD rats was 4.7 μ mol/L, i.e. similar to the known Km of NaPi-IIb (46). The *Km* value of the lower affinity component in diseased rats was 103.2 μ mol/L, which is equivalent to that of PiT-1 or PiT-2 (29). *Vmax* of phosphate uptake of the higher affinity component in diseased rats was apparently reduced compared to that of sham-operated rats (0.10 versus 0.33 pmol/μg protein/min, respectively).

The mRNA expression levels of 3 transporters in the upper intestine are shown in Table 17. Similar to the findings in adenine-induced CKD rats, PiT-1 or PiT-2 mRNA did not change in anti-Thy1 CKD rats. But again NaPi-IIb mRNA and protein were significantly decreased in diseased rats compared to normal rats, mirroring the decrease of phosphate uptake velocity (Figure 12). Injection of alfacalcidol also increased NaPi-IIb mRNA and protein back to normal levels in these animals (Table 18, Figure 8).

(A)

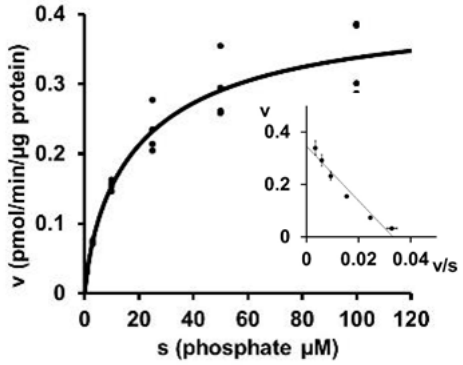

(B)

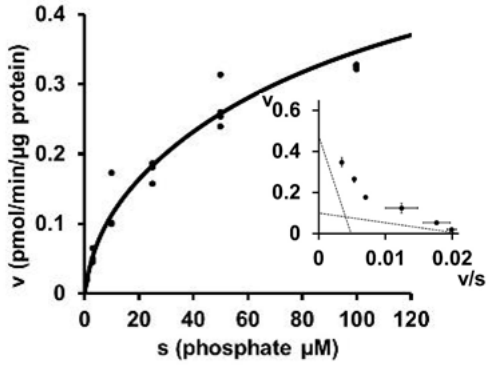

Figure 11. Phosphate uptake by intestinal BBMV in rats with anti-Thy1 CKD. Dots represent the actual values and the Michaelis-Menten curve was generated using JMP11.2.1. Inset shows an Eadie–Hofstee plot of the uptake. Each point represents the mean of three measurement points. Sham: sham-operated rats, CKD: anti-Thy1 CKD rats.

(A)

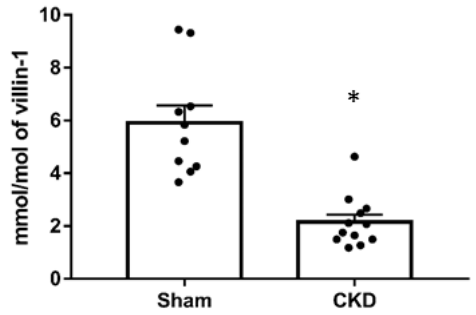

(B)

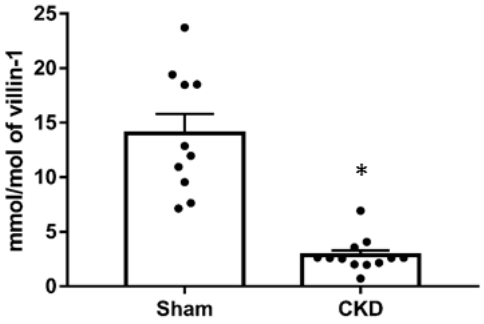

Figure 12. Changes in NaPi-IIb mRNA (A) or protein (B) expression level in upper intestine of rats with anti-Thy1 CKD. Values are normalized by villin-1 protein or mRNA, respectively. The actual values are represented as dots, and the columns represent mean + SE. *$p<0.05$, significant difference versus Normal (Student's t-test). Sham: sham-operated rats, CKD: anti-Thy1 CKD rats.

Table 15. Serum biochemistry and phosphate-related hormones in rats with anti-Thy1 CKD.

	Sham	CKD
Phosphate (mg/dL)	4.4 ± 0.1	9.6 ± 0.5[a]
Calcium (mg/dL)	10.3 ± 0.1	10.3 ± 0.1
BUN (mg/dL)	22.5 ± 0.3	128.3 ± 4.8[a]
Creatinine (mg/dL)	0.28 ± 0.00	1.83 ± 0.10[a]
FGF23 (pg/mL)	315 ± 13	19628 ± 6599[a]
Intact PTH (pg/mL)	4 ± 3	2782 ± 307[a]
Calcitriol (pg/mL)	120 ± 11	11 ± 1[a]

Values are expressed as mean ± SE (Sham: n=10, CKD: n=12). [a]$p<0.05$, significant difference versus normal control rats (Student's t- test). Sham, sham-operated rats; CKD: anti-Thy1 CKD rats.

Table 16. Kinetic parameters of phosphate uptake in BBMV of rats with anti-Thy1 CKD.

	Sham	CKD
K_m1 (μmol/L)	14.7 ± 3.0	4.7 ± 9.3
$V_{max}1$ (pmol/min/μg protein)	0.33 ± 0.02	0.10 ± 0.15
K_m2 (μmol/L)	-	103.2 ± 169.8
$V_{max}2$ (pmol/min/μg protein)	-	0.51 ± 0.20

Values are expressed as an estimate ± SE from non-linear regression analysis (n=4). Sham, sham-operated rats; CKD, anti-Thy1 CKD rats.

Table 17. Changes in NaPi-IIb, PiT-1, or PiT-2 mRNA expression level in upper intestine in rats with anti-Thy1 CKD.

	Sham	CKD
NaPi-IIb (mmol/mol villin-1)	5.9 ± 0.7	2.2 ± 0.3[a]
PiT-1 (mmol/mol villin-1)	19.8 ± 1.1	24.7 ± 2.8[a]
PiT-2 (mmol/mol villin-1)	0.27 ± 0.03	0.21 ± 0.02

Values are expressed as mean ± SE (Sham: n=10, CKD: n=12). [a]$p<0.05$, significant difference versus Sham (Student's t-test). Sham, sham-operated rats; CKD, anti-Thy1 CKD rats.

Table 18. Changes in NaPi-IIb, PiT-1, or PiT-2 mRNA expression level in upper intestine in rats with anti-Thy1 CKD after subcutaneous administration of alfacalcidol.

	Sham	CKD	VitD
NaPi-IIb (mmol/mol villin-1)	5.9 ± 0.7	2.2 ± 0.3[a]	25.8 ± 2.4[b]
PiT-1 (mmol/mol villin-1)	19.8 ± 1.1	24.7 ± 2.8[a]	17.0 ± 1.2[b]
PiT-2 (mmol/mol villin-1)	0.27 ± 0.03	0.21 ± 0.02	0.22 ± 0.03

Values are expressed as mean ± SE (n=10). [a]$p<0.05$, significant difference versus Sham, [b]$p<0.05$, significant difference versus CKD (Student's t-test). Sham: sham-operated rats, CKD: anti-Thy1 CKD rats, VitD: alfacalcidol via subcutaneous administration. Values were normalized via villin-1 mRNA.

4. Discussion

NaPi-IIb is believed to be the dominant transporter involved in active intestinal phosphate transport (15-18, 31-34). In the present study, I confirmed this in normal rats. However, in rats with CKD intestinal NaPi-IIb protein levels and intestinal phosphate absorption via NaPi-IIb decreased. Thus, our study establishes fundamental differences between normal and CKD rats, as well as differences in the regulation of intestinal phosphate transporters in CKD.

I analyzed the relationship between transporter expression and phosphate metabolism including intestinal phosphate absorption using healthy rats. In the present study, sodium-dependent phosphate uptake in normal rat intestine consisted of a single saturable component and its *Km* value was similar to that of NaPi-IIb (46). In agreement with previous findings (26), phosphate uptake (*Vmax*) in BBMV decreased with age and correlated with lower mRNA and protein expression levels of NaPi-IIb, identifying NaPi-IIb rather than PiT-1 or PiT-2 as the dominant transporter responsible for active phosphate uptake in rat intestine. NaPi-IIb is regulated by calcitriol in rodents and is increased by cholecalciferol administration or decreased by vitamin D receptor deletion (21, 25, 26, 62). In older rats NaPi-IIb protein and intestinal phosphate uptake capacity markedly decreased, consistent with the reduction of serum calcitriol and decrease in serum phosphate with age. A likely explanation is that in growing rats more phosphate is needed for bone growth and this demand decreases as growth slows down. My results thus indicate that intestinal phosphate uptake via NaPi-IIb changes with the physiological demand for phosphate in rats.

As the characteristics of intestinal phosphate absorption in CKD remain controversial, I analyzed the relationship between transporter expression and phosphate metabolism including intestinal phosphate absorption using 2 different CKD rat models. Both in adenine- and anti-Thy1-induced CKD in rats, serum phosphate significantly increased, and calcitriol significantly decreased, paralleled by a significant decrease in the intestinal mRNA and protein expression of NaPi-IIb. A strength of the present study is the consistency of the data in 2 fundamentally different CKD models: whereas adenine crystals directly injure renal proximal tubules (48), injection of anti-Thy1 antibody primarily damages glomeruli and tubular injury instead develops in a secondary fashion (49). As calcitriol is synthesized in renal proximal tubules, both models, despite being induced in different ways, resulted in reduced serum calcitriol levels. I confirmed the important role of calcitriol by showing that the injection of alfacalcidol restored intestinal NaPi-IIb mRNA and protein expression to normal even though kidney injury and hyperphosphatemia were not affected. Taken together, these data indicate that CKD-associated calcitriol deficiency suppresses intestinal

NaPi-IIb expression in rats with CKD. In contrast to calcitriol, cholecalciferol increased Na+-dependent phosphate uptake but only had a weak effect on NaPi-IIb expression (21). Unexpectedly, phosphate uptake into intestinal BBMV of rats in 2 CKD models consisted of two saturable components, which may reflect a compensatory response to the decreased NaPi-IIb mRNA and protein expression. The *Km* of the higher affinity component was 4.0 or 4.7 μmol/L in adenine CKD and anti-Thy1 CKD, respectively, which are equivalent to NaPi-IIb values. The phosphate uptake (Vmax) of the higher affinity component was apparently decreased in both CKD models compared with normal rats, which corresponds to the observed reduction in NaPi-IIb expression. These results indicate that the contribution of intestinal phosphate uptake via NaPi-IIb decreased in CKD rats. Whereas the Km of the lower affinity component was 166 or 103 μmol/L, respectively, which was equivalent to that of PiT-1 or PiT-2 (46, 47), Km and Vmax were similar in the anti-Thy1 and adenine CKD models, suggesting that CKD affects intestinal phosphate transporters independently of its origin. As the expression level of PiT-1 mRNA was much higher than PiT-2 mRNA in rats, PiT-1 might be responsible for the low affinity transport. However, in the intestine in 2 CKD rat models PiT-1 mRNA was not apparently increased compared with normal rats, which suggests PiT-1 protein is not regulated at the transcriptional level. However, I can not fully exclude that an as yet unknown transporter also contributes to intestinal phosphate absorption in rat CKD. Further studies are needed to better characterize the features of the lower affinity transporter(s) in rat CKD.

My results should be interpreted in the context of some limitations. Phosphate is absorbed in the small intestine by active transcellular transport and passive flow. Although the relative contribution of active versus passive pathway remains unknown, a pan-phosphate transporter inhibitor markedly ameliorated hyperphosphatemia in adenine and Thy1 induced CKD rats (49). Therefore, in the present study I focused on active transport. However, to understand the intestinal phosphate absorption rigorously, additional analyses e.g. using intestinal gut sacs would be needed. In addition, as my research is just based on rats, the question remains concerning extrapolation from rodents to humans. The expression levels of phosphate transporters in humans remain unknown and it will be necessary to study using human intestine to elucidate whether there are species differences in intestinal phosphate absorption.

In conclusion, my study identifies major differences between normal and CKD rats in the intestinal phosphate absorption system. NaPi-IIb appears to be the dominant intestinal phosphate transporter in young and healthy rats, and its expression is markedly affected by renal disease in that the contribution of NaPi-IIb to intestinal phosphate absorption is decreased in CKD and low affinity transporters such as PiT-1 gain in importance.

General Discussion

In the first part of this study (the chapter 1), there is a clear species difference in phosphate absorption in the small intestine, and it was considered that rats are the most suitable for extrapolating small intestinal phosphate absorption in humans from the viewpoint of phosphate absorption site.

In the second part of this study (the chapter 2), in normal rats, NaPi-IIb is mainly responsible for phosphate absorption, but the demand for phosphate decreased with aging, and the expression level of NaPi-IIb also decreased. While, renal injury, as the expression of NaPi-IIb in the small intestine decreases, the contribution of PiT-1, which has a lower affinity for phosphate than NaPi-IIb, for phosphate absorption in the small intestine increased relatively. From these results, NaPi-IIb was conventionally considered to be important for small intestinal phosphate absorption in rats, but a new mechanism of small intestinal phosphate absorption different from that of NaPi-IIb derived from PiT-1 was clarified. Therefore, it is important to inhibit not only NaPi-IIb but also PiT-1 / 2 mediated phosphate absorption in the suppression of phosphate absorption in the small intestine for the purpose of treating hyperphosphatemia.

The monkeys used in this study were characterized by phosphate metabolism compared to rats, dogs, and humans. The monkey used in this study, is a cynomolgus monkey, which is originally herbivore. Phosphate in plants is inorganic and does not require decomposition by ALP. In fact, the ALP activity in the small intestine of monkeys was low. In addition, it has already been reported that ALP activity is associated with NaPi-IIb expression level in the small intestine (49). And it is considered that the original diet of such species may be an important factor for phosphate transporters in the small intestine.

On the other hands, EOS789 inhibit several sodium-dependent phosphate transporters (NaPi-IIb, PiT-1, and PiT-2). This inhibitor dose-dependently increased the fecal phosphate excretion rate and inversely decreased the urinary phosphate excretion rate in normal rats, suggesting inhibition of intestinal phosphate absorption. In rats with adenine-induced hyperphosphatemia, EOS789 markedly decreased the serum phosphate, fibroblast growth factor-23, and intact parathyroid hormone, as biological markers, below values found in normal control rats (50).

However, the mechanism of phosphate absorption in humans is still unknown. I consider it an issue to examine the contribution rates of NaPi-IIb, PiT-1 and PiT-2 in the small intestine of healthy subjects, CKD, and dialysis patients. It was clear that major species differences for the expression of intestinal phosphate transporters were identified between humans and rats. Unlike in rats, PiT-2 appears to be the dominant intestinal Pi transporter in humans and its

expression was unaltered in patients with CKD. Thus, it was suggested that PiT-2 is a promising pharmacological target for the treatment of hyperphosphatemia in dialysis and/or CKD patients (51).

From the above examination, it was clarified that there are species differences in the phosphate absorption mechanism of the small intestine, and that the contribution rate of each transporter changes depending on aging or nephropathy. This indicates the existence of a different mechanism for the absorption of phosphate, which is important for living organisms, in the small intestine. And the inhibition of PiT is expected as therapeutic target for hyperphosphatemia.

Acknowledgements

I greatly appreciate Professor, Chikafumi Chiba, the University of Tsukuba, for supporting and guiding me in preparing this dissertation, and for coaching me with valuable discussion throughout my doctoral program.
I greatly thank all of the co-authors of the articles incorporated in this dissertation. The works were generated from the close collaboration between the doctors in Tokushima University Graduate School, RWTH Aachen University Hospital and the colleagues in Chugai Pharmaceutical Co., Ltd.
I also thank all the people who have been devoted to developing this research achievement.
Finally, I would like to appreciate my family for support during my time at the University of Tsukuba.

References

1. Murer H, Forster I, Hernando N, Lambert G, Traebert M, Biber J. 1999. Posttranscriptional regulation of the proximal tubule NaPi-II transporter in response to PTH and dietary P(i). Am J Physiol 277:F676-684.
2. Segawa H, Kawakami E, Kaneko I, Kuwahata M, Ito M, Kusano K, Saito H, Fukushima N, Miyamoto K. 2003. Effect of hydrolysis-resistant FGF23-R179Q on dietary phosphate regulation of the renal type-II Na/Pi transporter. Pflugers Arch 446:585-592.
3. Larsson T, Nisbeth U, Ljunggren O, Juppner H, Jonsson KB. 2003. Circulating concentration of FGF-23 increases as renal function declines in patients with chronic kidney disease, but does not change in response to variation in phosphate intake in healthy volunteers. Kidney Int 64:2272-2279.
4. Voormolen N, Noordzij M, Grootendorst DC, Beetz I, Sijpkens YW, van Manen JG, Boeschoten EW, Huisman RM, Krediet RT, Dekker FW, group Ps. 2007. High plasma phosphate as a risk factor for decline in renal function and mortality in pre-dialysis patients. Nephrol Dial Transplant 22:2909-2916.
5. Tentori F, Blayney MJ, Albert JM, Gillespie BW, Kerr PG, Bommer J, Young EW, Akizawa T, Akiba T, Pisoni RL, Robinson BM, Port FK. 2008. Mortality risk for dialysis patients with different levels of serum calcium, phosphorus, and PTH: the Dialysis Outcomes and Practice Patterns Study (DOPPS). Am J Kidney Dis 52:519-530.
6. Fournier A MP, Ben Hamida F, el Esjer N, Shenovda M, Ghazali A, Bouzernidj M, Achard JM, Westeel PF. 1992. Use of alkaline calcium salts as phosphate binder in uremic patients. Kidney Int Suppl 38:50-61.
7. Pieper AK, Haffner D, Hoppe B, Dittrich K, Offner G, Bonzel KE, John U, Frund S, Klaus G, Stubinger A, Duker G, Querfeld U. 2006. A randomized crossover trial comparing sevelamer with calcium acetate in children with CKD. Am J Kidney Dis 47:625-635.
8. Sheikh MS, Maguire JA, Emmett M, Santa Ana CA, Nicar MJ, Schiller LR, Fordtran JS. 1989. Reduction of dietary phosphorus absorption by phosphorus binders. A theoretical, in vitro, and in vivo study. J Clin Invest 83:66-73.
9. Floege J, Covic AC, Ketteler M, Mann JF, Rastogi A, Spinowitz B, Chong EM, Gaillard S, Lisk LJ, Sprague SM, Sucroferric Oxyhydroxide Study G. 2015. Long-term effects of the iron-based phosphate binder, sucroferric oxyhydroxide, in dialysis patients. Nephrol Dial Transplant 30:1037-1046.

10. Hutchison AJ, Wilson RJ, Garafola S, Copley JB. 2016. Lanthanum carbonate: Safety data after 10 years. Nephrology (Carlton) 21:987-994.
11. Mineo H, Morikawa N, Ohmi S, Ishida K, Machida A, Kanazawa T, Chiji H, Fukushima M, Noda T. 2010. Ingestion of potato starch containing esterified phosphorus increases alkaline phosphatase activity in the small intestine in rats. Nutr Res 30:341-347.
12. Giral H, Caldas Y, Sutherland E, Wilson P, Breusegem S, Barry N, Blaine J, Jiang T, Wang XX, Levi M. 2009. Regulation of rat intestinal Na-dependent phosphate transporters by dietary phosphate. Am J Physiol Renal Physiol 297:F1466-1475.
13. Kirchner S, Muduli A, Casirola D, Prum K, Douard V, Ferraris RP. 2008. Luminal fructose inhibits rat intestinal sodium-phosphate cotransporter gene expression and phosphate uptake. Am J Clin Nutr 87:1028-1038.
14. Peerce BE, Fleming RY, Clarke RD. 2003. Inhibition of human intestinal brush border membrane vesicle Na^+-dependent phosphate uptake by phosphophloretin derivatives. Biochem Biophys Res Commun 301:8-12.
15. Ikuta K, Segawa H, Sasaki S, Hanazaki A, Fujii T, Kushi A, Kawabata Y, Kirino R, Sasaki S, Noguchi M, Kaneko I, Tatsumi S, Ueda O, Wada NA, Tateishi H, Kakefuda M, Kawase Y, Ohtomo S, Ichida Y, Maeda A, Jishage KI, Horiba N, Miyamoto KI. 2018. Effect of Npt2b deletion on intestinal and renal inorganic phosphate (Pi) handling. Clin Exp Nephrol 22:517-528.
16. Sabbagh Y, O'Brien SP, Song W, Boulanger JH, Stockmann A, Arbeeny C, Schiavi SC. 2009. Intestinal npt2b plays a major role in phosphate absorption and homeostasis. J Am Soc Nephrol 20:2348-2358.
17. Xu H, Bai L, Collins JF, Ghishan FK. 1999. Molecular cloning, functional characterization, tissue distribution, and chromosomal localization of a human, small intestinal sodium-phosphate (Na+-Pi) transporter (SLC34A2). Genomics 62:281-284.
18. Hilfiker H, Hattenhauer O, Traebert M, Forster I, Murer H, Biber J. 1998. Characterization of a murine type II sodium-phosphate cotransporter expressed in mammalian small intestine. Proc Natl Acad Sci U S A 95:14564-14569.
19. Larsson TE, Kameoka C, Nakajo I, Taniuchi Y, Yoshida S, Akizawa T, Smulders RA. 2018. NPT-IIb Inhibition Does Not Improve Hyperphosphatemia in CKD. Kidney Int Rep 3:73-80.
20. Giral H, Cranston D, Lanzano L, Caldas Y, Sutherland E, Rachelson J, Dobrinskikh E, Weinman EJ, Doctor RB, Gratton E, Levi M. 2012. NHE3 regulatory factor 1 (NHERF1) modulates intestinal sodium-dependent phosphate transporter (NaPi-2b) expression in apical microvilli. J Biol Chem 287:35047-35056.

21. Hattenhauer O, Traebert M, Murer H, Biber J. 1999. Regulation of small intestinal Na-P(i) type IIb cotransporter by dietary phosphate intake. Am J Physiol 277:G756-762.
22. Segawa H, Kaneko I, Yamanaka S, Ito M, Kuwahata M, Inoue Y, Kato S, Miyamoto K. 2004. Intestinal Na-P(i) cotransporter adaptation to dietary P(i) content in vitamin D receptor null mice. Am J Physiol Renal Physiol 287:F39-47.
23. Layunta E, Pastor Arroyo EM, Kagi L, Thomas L, Levi M, Hernando N, Wagner CA. Intestinal 2019. Response to Acute Intragastric and Intravenous Administration of Phosphate in Rats. Cell Physiol Biochem 52:838-849.
24. Stieger B, Murer H. 1983. Heterogeneity of brush-border-membrane vesicles from rat small intestine prepared by a precipitation method using Mg/EGTA. Eur J Biochem 135:95-101.
25. Brown AJ, Zhang F, Ritter CS. 2012. The vitamin D analog ED-71 is a potent regulator of intestinal phosphate absorption and NaPi-IIb. Endocrinology 153:5150-5156.
26. Xu H, Bai L, Collins JF, Ghishan FK. 2002. Age-dependent regulation of rat intestinal type IIb sodium-phosphate cotransporter by 1,25-$(OH)_2$ vitamin D_3. Am J Physiol Cell Physiol 282:C487-493.
27. Candeal E, Caldas YA, Guillen N, Levi M, Sorribas V. 2017. Intestinal phosphate absorption is mediated by multiple transport systems in rats. Am J Physiol Gastrointest Liver Physiol 312:G355-G366.
28. Walton J, Gray TK. 1979. Absorption of inorganic phosphate in the human small intestine. Clin Sci (Lond) 56:407-412.
29. Dhayat NA, Ackermann D, Pruijm M, Ponte B, Ehret G, Guessous I, Leichtle AB, Paccaud F, Mohaupt M, Fiedler GM, Devuyst O, Pechere-Bertschi A, Burnier M, Martin PY, Bochud M, Vogt B, Fuster DG. 2016. Fibroblast growth factor 23 and markers of mineral metabolism in individuals with preserved renal function. Kidney Int 90:648-657.
30. J.B.Anderson J. 1991. Nutritional biochemistry of calcium and phosphate. J Nutr Biochem 2:300-307.
31. Marks J. The role of Slc34a2 in intestinal phosphate absorption and phosphate homeostasis. *Pflugers Arch* 2019; 471: 165-173
32. Lederer E, Wagner CA. Clinical aspects of the phosphate transporters NaPi-IIa and NaPi-IIb. Mutations and disease associations. *Pflugers Arch* 2019; 471: 137-148
33. Wagner CA, Hernando N, Forster IC et al. The Slc34 family of sodium-dependent phosphate transporters. *Pflugers Arch* 2014; 466: 139-153
34. Ohi A, Hanabusa E, Ueda O et al. Inorganic phosphate homeostasis in sodium-dependent phosphate cotransporter Npt2b(+)/(-) mice. *Am J Physiol Renal Physiol*

2011; 301: F1105-1113
35. Fouque D, Pelletier S, Mafra D et al. Nutrition and chronic kidney disease. *Kidney Int* 2011; 80: 348-357
36. Block GA, Klassen PS, Lazarus JM et al. Mineral metabolism, mortality, and morbidity in maintenance hemodialysis. *J Am Soc Nephrol* 2004; 15: 2208-2218
37. Kanbay M, Goldsmith D, Akcay A et al. Phosphate-the silent stealthy cardiorenal culprit in all stages of chronic kidney disease. A systematic review. Blood Purif 2009; 27: 220-230
38. Palmer SC, Hayen A, Macaskill P et al. Serum levels of phosphorus, parathyroid hormone, and calcium and risks of death and cardiovascular disease in individuals with chronic kidney disease. A systematic review and meta-analysis. *JAMA* 2011; 305: 1119-1127
39. Bleyer AJ, Burke SK, Dillon M et al. A comparison of the calcium-free phosphate binder sevelamer hydrochloride with calcium acetate in the treatment of hyperphosphatemia in hemodialysis patients. *Am J Kidney Dis* 1999; 33: 694-701
40. Aniteli TM, de Siqueira FR, Dos Reis LM et al. Effect of variations in dietary Pi intake on intestinal Pi transporters (NaPi-IIb, Pit-1, and Pit-2) and phosphate-regulating factors (PTH, FGF-23, and MEPE). *Pflugers Arch* 2018; 470: 623-632
41. Kamiie J, Ohtsuki S, Iwase R et al. Quantitative atlas of membrane transporter proteins. Development and application of a highly sensitive simultaneous LC/MS/MS method combined with novel in-silico peptide selection criteria. *Pharm Res* 2008; 25: 1469-1483
42. Cheng QL, Orikasa M, Morioka T et al. Progressive renal lesions induced by administration of monoclonal antibody 1-22-3 to unilaterally nephrectomized rats. *Clin Exp Immunol* 1995; 102: 181-185
43. Ichida Y, Hosokawa N, Takemoto R et al. Significant species differences in intestinal phosphate absorption between dogs, rats, and monkeys. *J Nutr Sci Vitaminol (Tokyo)* 2020; 66: 60-67
44. Takahashi K, Masuda S, Nakamura N et al. Upregulation of H(+)-peptide cotransporter PEPT2 in rat remnant kidney. *Am J Physiol Renal Physiol* 2001; 281: F1109-1116
45. Kamiie J OS TTUTNC, assignee. Method of quantifying membrane protein by using mass spectrometer. JP patent 4670060 2011; Jan 28.
46. Forster IC, Virkki L, Bossi E et al. Electrogenic kinetics of a mammalian intestinal type IIb Na(+)/P(i) cotransporter. *J Membr Biol* 2006; 212: 177-190
47. Ravera S, Virkki LV, Murer H et al. Deciphering pit transport kinetics and substrate specificity using electrophysiology and flux measurements. *Am J Physiology Cell Physiol* 2007; 293: C606-620
48. Katsumata K, Kusano K, Hirata M et al. Sevelamer hydrochloride prevents ectopic

calcification and renal osteodystrophy in chronic renal failure rats. *Kidney Int* 2003; 64: 441-450

49. Sasaki S, Segawa H, Hanazaki A et al. A Role of Intestinal Alkaline Phosphatase 3 (Akp3) in Inorganic Phosphate Homeostasis. *Kidney Blood Press Res* 2018;43(5):1409-1424
50. Tsuboi Y, Ohtomo S, Ichida Y et al. EOS789, a novel inhibitor of multi-phosphate transporters, is effective for the treatment of chronic kidney disease–mineral bone disorder ilure rats. *Kidney Int* 2020; 66: 60-67
51. Gallant K, Stremke E, Trevino L et al. EOS789, a broad-spectrum inhibitor of phosphate transport, is safe with an indication of efficacy in a phase 1b randomized crossover trial in hemodialysis patients. *Kidney Int* 2021; 99(5):1225-1233

List of Publications

The chapter 1

Yasuhiro Ichida, Naoto Hosokawa, Ryushi Takemoto, Takafumi Koike, Tasuku Nakatogawa, Mayumi Hiranuma, Hitoshi Arakawa, Yukihito Miura, Hiroko Azabu, Shuichi Ohtomo, Naoshi Horiba.

Significant Species Differences in Intestinal Phosphate Absorption between Dogs, Rats, and Monkeys.

J Nutr Sci Vitaminol (Tokyo). 2020;66(1):60-67.

The chapter 2

Yasuhiro Ichida, Shuichi Ohtomo, Tessai Yamamoto, Naoaki Murao, Yoshinori Tsuboi, Yoshiki Kawabe, Hiroko Segawa, Naoshi Horiba, Ken-ichi Miyamoto, Jürgen Floege.

Evidence of an intestinal phosphate transporter alternative to type IIb sodium-dependent phosphate transporter in rats with chronic kidney disease.

Nephrol Dial Transplant. 2021; 36(1): 68-75.